JSEE Vol. 27, No. 1, 2025 DOI: 10.48303/jsee.2024.2034260.1110

Research Paper

Effect of Composite Action on Seismic Response of Steel Structures with Dampers Designed by the DDBD Method

Seyed Behdad Alehojjat[1], Masood Yakhchalian[2] and Omid Bahar[3]*

1. Researcher in Structural Engineering, Department of Civil Engineering, Qa. C., Islamic Azad University, Qazvin, Iran
2. Assistant Professor, Department of Civil Engineering, Qa. C., Islamic Azad University, Qazvin, Iran,
*Corresponding Author; email: ma.yakhchalian@iau.ac.ir
3. Associate Professor, Structural Engineering Research Center, International Institute of Earthquake Engineering & Seismology (IIEES), Tehran, Iran

Received: 01/07/2024
Revised: 27/09/2024
Accepted: 29/09/2024

Keywords:
Direct displacement-based design; Inter-story drift ratio; Residual inter-story drift ratio; Composite action; Linear fluid viscous damper

ABSTRACT

This paper investigates two important engineering demand parameters for assessing seismic performance of steel moment resisting frames equipped with linear fluid viscous dampers designed using the modified direct displacement-based design (DDBD) method. These parameters include the inter-story drift ratio (IDR) and the residual inter-story drift ratio (RIDR). For this aim, nonlinear dynamic time history analyses are performed at two seismic hazard levels, involving the design basis earthquake (DBE) and the maximum considered earthquake (MCE). The effects of panel zone flexibility and gravity framing are modeled in the analyses. In addition, the effect of considering and neglecting composite action on gravity framing and beam elements in moment resisting frames is investigated. The results show that in both cases, the structures designed using the modified DDBD method could acceptably meet the performance target IDR limit. Additionally, it is shown that accounting for the effect of composite action leads to a reduction of about 4% in the maximum value of mean IDRs at both the DBE and MCE hazard levels. However, an increase of up to 12% is obtained for the maximum value of median RIDRs at the MCE level when the composite action is considered.

How to cite the article:
Alehojjat , S.B., Yakhchalian, M., & Bahar, O. (2025). Effect of Composite Action on Seismic Response of Steel Structures with Dampers Designed by the DDBD Method. *Journal of Seismology and Earthquake Engineering*, *27*(1), 89-102. doi: 10.48303/jsee.2024.2034260.1110

1. Introduction

Since the deformations control the structural damage resulted in the earthquakes, displacement-based design (DBD) approaches were introduced instead of the conventional force-based design (FBD) approaches. In fact, DBD approaches have considered a real correlation between displacement and damage extent (Rahgozar & Rahgozar, 2020). One of the most applicable and highly developed approaches is the direct displacement-based design (DDBD) method (Priestley, 1993; Priestley et al., 2007). This method proposes a straight-forward procedure and has also been developed by many researchers to design different lateral resisting systems such as steel moment resisting frame (MRF) system (e.g., Sulivan et al., 2018; Shakeri and Dadkhah, 2021), buckling-restrained brace (BRB) system (Farahani and Akhaveissy, 2022; Kalapodis et al., 2022), rocking core system (Rahgozar and Rahgozar, 2020; Hu et al., 2023), etc. Fluid viscous dampers are the passive control devices that can improve the seismic performance of structures. Structures equipped with fluid viscous dampers were designed by Sullivan and Lago (2012) using the mentioned method. After then, several research works have been conducted to improve the method, such as Moradpour and Dehestani (2019), Noruzvand et al. (2020), Alehojjat et al. (2021, 2024).

To investigate the performance of a structure after an earthquake, the residual inter-story drift ratio (RIDR) is an important index for structural resilience. In fact, this parameter can determine whether a structure should be demolished, retro-fitted, or repaired. Different research studies have presented values for this parameter to quantify the necessity of repairing of structures (e.g., Erochko et al., 2011; FEMA P58, 2018). As an instance, FEMA P58 proposes four damage states for a structure according to the maximum value of median RIDRs. The lowest damage state is related to the non-structural components and the highest damage state corresponds to the near collapse of structure. Also, several studies have been conducted to predict the RIDR demand in different structural systems, such as Asgarkhani et al. (2020), Yakhchalian & Yakhchalian (2023), Arab and Yakhchalian (2022) and Alehojjat et al. (2023).

Most of seismic design codes (e.g., US and Canada codes) do not consider the contribution of the interior gravity framing system in steel structures to their capacities. Shear tap connections are the most common and practical type of beam-to-column connection in these structures. They are modeled as pinned connections with zero flexural stiffness and strength (Elkady & Lignos, 2015, Yakhchalian & Yakhchalian, 2023). Studies conducted by Liu and Astaneh-Asl (2000, 2004), Leon et al. (1998) and Green et al. (2004) indicated that shear tap connections dedicate up to 20% of the plastic flexural strength of the gravity beam to themselves. However, considering the effect of composite action due to concrete slab may also increase the mentioned value to 50%. Therefore, the seismic behavior of structures can be influenced by implementing a large number of tab connections in the gravity frames.

In this paper, the seismic performance level of two mid-rise steel structures, designed by the DDBD method with applying modifications proposed by Noruzvand et al. (2020), (2021) and Alehojjat et al. (2021) is investigated. To this end, panel zone flexibility and the effect of gravity framing are modeled in the designed structures with and without considering the effect of composite action. Additionally, the values of mean IDR and median RIDR obtained from nonlinear analyses are compared at the maximum considered earthquake (MCE) and design basis earthquake (DBE) hazard levels.

2. DDBD Method for Steel Structures with Damper

2.1. Conventional Method

The main concept of DDBD is to employ a single-degree-of-freedom (SDOF) structure instead of a multi-degree-of-freedom (MDOF) structure. Therefore, some parameters, including the design displacement (Δ_d), effective mass (m_e), effective height (H_e), yield rotation (θ_y) yield displacement (Δ_y), and ductility demand (μ) should first be determined. Equations (1) to (7) present the required relations for these parameters.

$$\Delta_i = \omega_\theta \theta_c h_i \left(\frac{4H_n - h_i}{4H_n - h_1} \right) \quad (1)$$

$$\Delta_d = \frac{\sum_{i=1}^{n}(m_i\Delta_i^2)}{\sum_{i=1}^{n}(m_i\Delta_i)} \quad (2)$$

$$m_e = \frac{\sum_{i=1}^{n}(m_i\Delta_i)}{\Delta_d} \quad (3)$$

$$H_e = \frac{\sum_{i=1}^{n}(m_i\Delta_i h_i)}{\sum_{i=1}^{n}(m_i\Delta_i)} \quad (4)$$

$$\theta_y = 0.65\varepsilon_y \frac{L_b}{h_b} \quad (5)$$

$$\Delta_y = \theta_y H_e \quad (6)$$

$$\mu = \frac{\Delta_d}{\Delta_y} \quad (7)$$

where the story drift limit (target performance level) is shown by θ_c, Δ_i is the design displacement of story i, h_i and H_n are the height of i^{th} and last floor from the base, respectively. ω_θ considers the effects of higher modes. m_i denotes the seismic mass of the i^{th} floor and n is the number of floors. L_b and h_b are the beam length and depth, respectively, and ε_y is the yield strain of steel. For a detailed calculation of these parameters and other parameters in this section, readers can refer to Sullivan and Lago (2012), Noruzvand et al. (2020) and Alehojjat et al. (2021). The next step is to obtain the equivalent viscous damping (ξ_{eq}). Sullivan and Lago (2012) proposed Equation (8) to calculate ξ_{eq} for frames with viscous dampers. In this equation, $\xi_{eq,\ frame}$ consists of the elastic damping (ξ_{el}) equal to 0.05 and the hysteretic damping of the steel MRFs (ξ_{hyst}) as defined in Equation (9). Also, the added damping based on the fluid viscous dampers (ξ_{FVD}) is determined by Equation (10).

$$\xi_{eq} = \xi_{eq,\ frame} + \xi_{FVD} \quad (8)$$

$$\xi_{hyst} = 0.71\left(\frac{\mu - 1}{\mu\pi}\right) \quad (9)$$

$$\xi_{FVD} = \frac{\lambda\beta}{2} \quad (10)$$

where the portion of the story shear that should be carried out by dampers in each story is shown by parameter β, and α is the velocity exponent of the damper. The design parameter λ relates to α and is equal to 1.0 for the linear damper.

Knowing the equivalent viscous damping of the SDOF structure and the design displacement, the effective period (T_{eff}) can be read by the reduced displacement spectrum according to the value of the calculated equivalent viscous damping. After that, the design base shear (V_b) is obtained. The lateral distribution of the obtained base shear along the height of the structure leads to calculating the required moments in each level for beams ($M_{b,i}$), internal columns ($M_{c,int}$) and external columns ($M_{c,ext}$) as follows:

$$M_{b,i} = \frac{(2K_iV_i + V_{i+1})h_s}{4n_b} \quad (11)$$

$$M_{col,\text{int}} = \frac{(1 - K_1)h_sV_b}{n_b} \quad (12)$$

$$M_{col,ext} = \frac{M_{col,\text{int}}}{2} \quad (13)$$

where V_i and h_i are the each story shear at level i and inter-story height, respectively. n_b is defined as the number of bays in the frame. The parameter K_1 is the factor that determines the point of contra-flexure in the base floor and is equal to 0.4. For other floors, it should be considered equal to 0.5. It is noting that capacity design for columns is also done to consider strong column-weak beam criteria. After selecting the member sections, the damper constants (C_i) are calculated as follows:

$$C_i = \frac{F_{d,i}T_e^{\alpha}}{2_{\pi}^{\alpha}\Delta_{d,i}^{\alpha}} \quad (14)$$

$$F_{d,i} = \beta V_i \quad (15)$$

$$\Delta_{d,i} = (\Delta_i - \Delta_{i-1})\cos\theta_{FVD} \quad (16)$$

where $F_{d,i}$ and $\Delta_{d,i}$ are the damper force and damper displacement at level i, respectively. Δ_i denotes the frame displacement at level i and the angle between the damper and horizontal inclination is shown by θ_{FVD}. The parameter α is the velocity exponent of the damper and shows the nonlinearity of the damper response. For the linear damper, α is set to 1.0.

2.2. Modified Method

In order to economically design structures

equipped with viscous dampers, two modifications are considered in the conventional method (Noruzvand et al., 2019; Alehojjat et al., 2021). The effects of interaction between the structure ductility demand and extra added damping related to fluid viscous dampers as well as a modification factor due to the ratio of pseudo-spectral velocity to spectral velocity (γ). Therefore, the equivalent viscous damping equation in low to mid-rise structures is modified by Equation (17). It is noted that the mentioned equation is similar to the equivalent lateral force (*ELF*) procedure presented in ASCE 7 (2017).

$$\xi_{eq} = \xi_{el} + \xi_{hyst} + \xi_{FVD}\left(\mu\right)^{1-\frac{\alpha}{2}} \tag{17}$$

Moreover, in the equation for determining the damper constants (i.e., Equation 14), the parameter γ is also considered as follows:

$$C_i = \frac{\gamma F_{d,i} T_e^{\alpha}}{2_{\pi}^{\alpha} \Delta_{d,i}^{\alpha}} \tag{18}$$

In order to determine γ, there are two methods. The first method is to obtain the velocity and pseudo-velocity spectrum for each damping value, and the second method is to calculate the factor using the equation proposed by Papagiannopoulos et al. (2013) as follows:

$$\gamma = \frac{S_{pv}}{S_v} = \frac{1}{a + bt + c\xi + dT^2 + e\xi^2 + fT\xi} \tag{19}$$

where the parameters *a*, *b*, *c*, *d*, *e*, and *f* are determined based on these properties, the site class of the structure's location, six possible combinations among the magnitude of the earthquake and Joyner-Boore distance and to be far or near field of the earthquake. For simplicity, Noruzvand et al. (2021) determined γ via the average values of the six combinations for each site class. In the present study, these average values were used.

3. Properties of the Structures Considered and Analyses

The modified DDBD method is implemented to design 3- and 6-story steel moment frames equipped with linear fluid viscous dampers. Similar to Kitayama and Constantinou (2018), it was assumed that the structures are located on a site with high seismicity in California (latitude 37.8814°N, and longitude 122.08°W), which is classified as site class *D* according to ASCE 7 (2017). The short-period MCE response spectral acceleration of the site (S_{MS}) and 1-s period MCE spectral response acceleration (S_{M1}) are 1.5 g and 0.9 g, respectively. These values for the DBE hazard level are 1.0 g and 0.6 g, respectively. Also, long-period transition period (T_L) is 8.0 s. The lateral resisting system of the structures consists of four perimeter frames that are configured as MRFs. Figure (1a) shows the plan of the buildings. All columns, except the MRFs, were modeled as equivalent gravity frame (EGF) as shown in Figure (1b). Also, the heights of the stories for the 3-story structure are indicated in the mentioned figure. The dead load values of 3.35 kN/m^2 and 1.68 kN/m^2 were assumed for floors and roof, respectively. For the live load, the values of 1.68 kN/m^2 and 0.96 kN/m^2 were considered, for floors and roof, respectively. Moreover, the

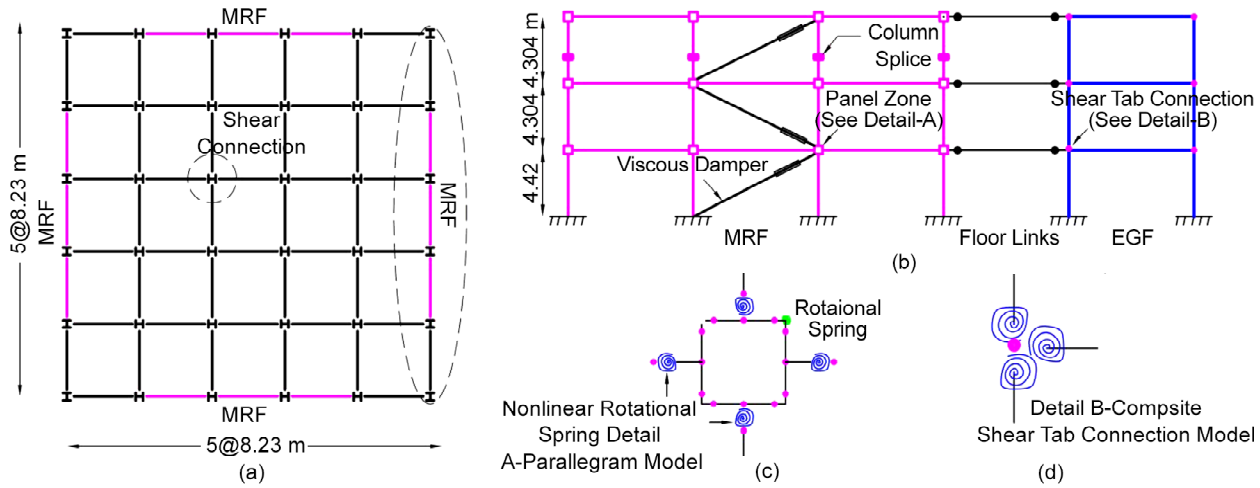

Figure 1. (a) Plan view, (b) typical elevation, and (c) panel zone modeling (d) shear tab connection for the considered structures.

value of 1.2 kN/m^2 was determined for the cladding load (Kitayama & Constantinou, 2016). To consider the effect of composite action, a thickness of 0.05 m and 0.075 m was employed for the concrete slab and rips, respectively. *W* sections were applied for beams and columns. The modulus of elasticity for the structural elements was assumed to be 200 GPa. The yield stress of 345 MPa was assumed for W sections. The expected yield stress was taken to 1.1 times the yield stress.

To create two-dimensional frame models and perform nonlinear dynamic time history analyses, the OpenSees (2020) program was used (Elkady, 2022). The P-Δ effects of gravity framing in the structures as well as the strength and stiffness of the gravity framing system (i.e., shear tab connections in the case of considering the effect of composite action) were accounted for by modeling the EGF that consists of elastic elements with high rigidity and it was linked to the frames as shown in Figure (1b) and (1d). To simulate the nonlinear behavior of the MRFs, concentrated plasticity approach was applied in beams and columns. In addition, a parallelogram model (Gupta & Krawinkler, 1999; Elkady & Lignos, 2014) was employed to explicitly simulate the panel zone flexibility modeled as shown in Figure (1c). The schematic presentation of the backbone curve utilized for the panel zone simulation is illustrated in Figure (2), where V_y and V_p are the yield shear and the plastic shear forces, respectively. Yield distortion is denoted by γ_y and the distortion corresponding to plastic shear force is γ_p. The slopes of the second and third lines in the backbone curve present the post-yield shear stiffness of panel zone (K_p) and the reduced stiffness of panel zone after plastic shear force (K_{sh}), respectively (for a more detailed explanation of the parameters, readers can refer to Gupata and Krawinkler, 1999). Equations required for modeling panel zone parameters are presented in Table (1). Since the cyclic behavior of shear tab connections is determined using moment-rotation hysteretic response with pinching, in the OpenSees program, the pinching 4 material was used to simulate this effect. Figure (3) schematically presents the effect of composite

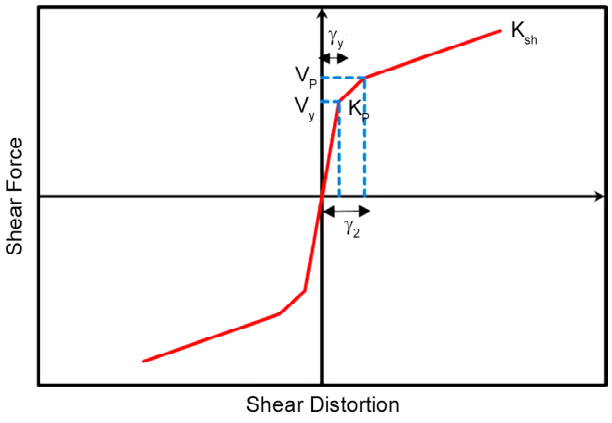

Figure 2. Schematic symmetric backbone curve for modeling panel zone.

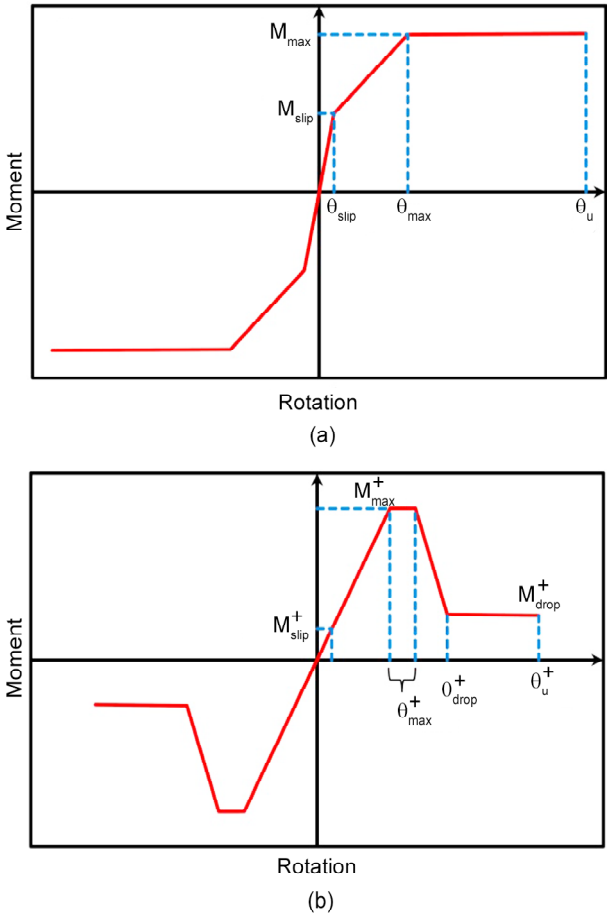

Figure 3. Schematic backbone curve for modeling shear tab connection in gravity frame (a) without composite action (b) with composite action.

Table 1. Equations and parameters required for modeling panel zone backbone curve.

M_y	M_y^-	M_y^+	d_e^+	V_P	M_P^+
$V_y\ d_e$	$V_y\ d_e$	$V_y\ d_e^+$	d_b | d_{rib} | $0.5t_s$-$0.5t_f$	V_y | $K_P\ (\gamma_2$-$\gamma_1)$	$V_p\ d_e^+$

d_e = Effective depth of beam, d_b = Depth of beam
d_{rib} = Depth of ribbed section, t_s = Concrete slab depth, t_f = Thickness of the beam flange

action on the behavior of shear tab connections. In this figure, M_{slip} presents the flexural strength at the point of bolt slip occurrence. θ_{slip} is the chord rotation corresponding to M_{slip}. The maximum flexural strength and the corresponding rotation are shown by M_{max} and θ_{max}, respectively. θ_u indicates the rotation at which the connection failure is reached. M_{drop} corresponds to the reduced flexural strength of the connection after slab concrete crushing. θ_u is the chord rotation at which M_{drop} occurs (for a more detailed explanation of the parameters, readers can refer to Elkady and Lignos, 2015). The Ibarra-Medina-Krawinkler (IMK) model (2005) was applied for rotational springs of beam elements in MRFs, as illustrated in Figure (4a). To consider asymmetric hysteretic behavior for beam elements in MRF because of the composite action, residual strength and ductile tearing, the modified IMK model, see Figure (4b), developed by Lignos & Krawinkler (2011), was applied. In this figure, M_y denotes the effective yield moment, M_c is the capping moment and the residual moment is indicated by M_r. The precapping rotation and the post capping rotation are denoted by θ_p and θ_{pc}, respectively. According to the research study done by Elkady & Lignos (2015), Table (2) shows the parameters required for modeling the backbone curves of shear tab connections presented in Figures (3) and (4). In addition, the model recommended by Lignos et al. (2019) was used for column rotational springs to consider the strength and stiffness deterioration of steel columns under seismic loading. The location of column splices was assumed to be at the middle of the columns and these were modeled by rigid springs (with a large elastic stiffness of 109 for translation along x and y axes as well as rotation about z axe). The truss element command was applied to model viscous dampers. It is noted that the rigid diaphragm was also defined in the model. The static gravity analysis with load combination

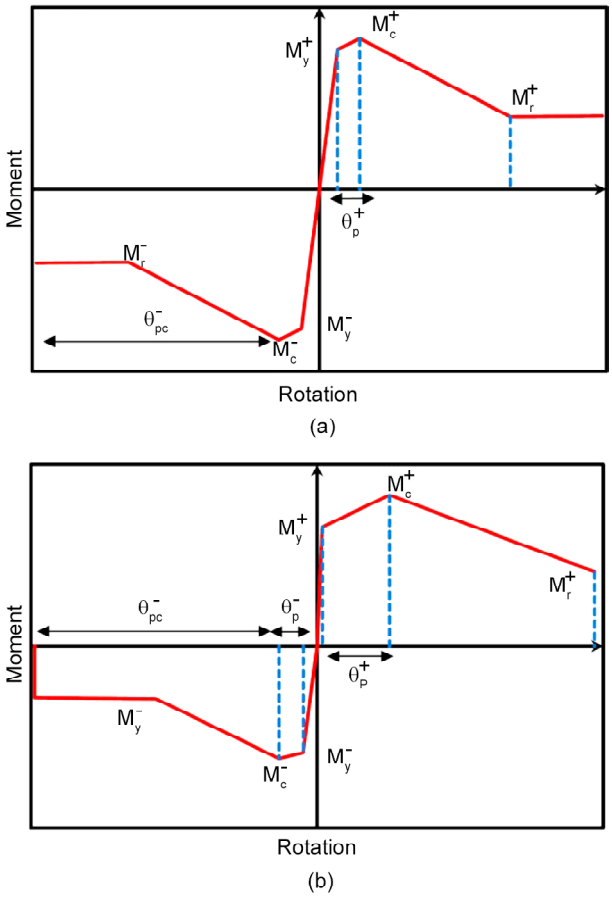

Figure 4. Schematic backbone curve for modeling beam elements in MRF (a) without composite action (b) with composite action.

of (Dead + 0.25Live) was conducted on the structure before performing the seismic nonlinear analysis a ccording to ASCE 41 (2017).

To perform the nonlinear dynamic time history analyses, the SAC project (Somerville, 1997) scaled ground motion records for Los Angeles, including 20 records, were used. Since the average of pseudo response spectra of La 1-20 records does not match with the MCE response spectrum for the site considered, the records were scaled by a factor of 1.25. As can be seen in Figure (5), the average pseudo-acceleration spectra of the mentioned records are properly matched with the corresponding ASCE 7 response spectrum at the MCE hazard level.

Table 2. Parameters required for modeling shear tab backbone curve (Yakhchalian & Yakhchalian, 2023).

	$\frac{M_{max}}{M_p}$	$\frac{M_{slip}}{M^+_{max}}$	$\frac{M^-_{max}}{M^+_{max}}$	$\frac{M^+_{drop}}{M^+_{max}}$	$\frac{M^-_{drop}}{M^-_{max}}$	θ_{slip}	θ'_{max}	θ^-_{max}	θ'_{drop}	θ^-_{drop}
Neglecting Composite Action	0.13	0.5	1.0	-	-	0.004	0.05	0.05	-	-
Considering Composite Action	0.35	0.25	0.64	0.53	0.54	0.004	0.02-0.039	0.012-0.03	0.04	0.055

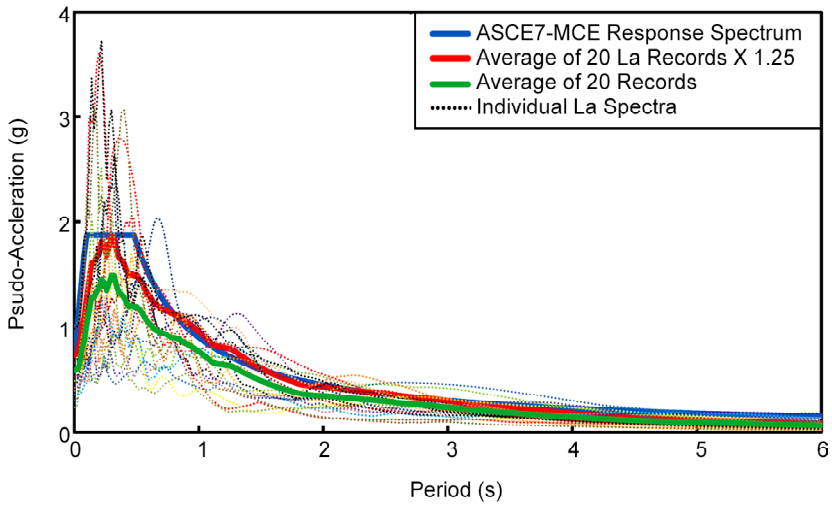

Figure 5. MCE Response spectrum versus average spectrum of considered earthquakes with and without applying constant factor of 1.25.

4. Structures Designed by Modified DDBD

The design parameters of the two structures according to the modified DDBD method are presented in this section. The initial design parameters of the SDOF structure are given in Table (3). It is noted that the value of 3.0% was determined for the target IDR limit at the MCE hazard level based on ASCE 7 (2017).

Furthermore, the value of 0.3 was assumed for β. The required parameters for designing structural elements and dampers are presented for the 3-story and 6-story structures in Tables (4) and (5), respectively.

Following the design procedure discussed in Section 2, the final sections for the beams and columns are shown in Figure (6). It is worth mentioning that these structures were designed for the MCE hazard level.

Table 3. SDOF parameters for the considered structures.

Structure	Δ_d (m)	m_e (ton)	H_e (m)	Δ_y (m)	μ	ξ_{eq}	T_e (s)	V_b (kN)
3-Story	0.238	663	9.04	0.204	1.17	0.244	1.82	1.92
6-Story	0.437	1360	17.20	0.349	1.25	0.265	3.46	2.01

Table 4. Member and damper design parameters for the 3-story structure.

Level	F_i (kN)	V_i (kN)	$M_{b,i}$ (kN.m)	$M_{col,int}$ (kN.m)	$M_{col,ext}$ (kN.m)	F_{di} (kN)	C_i (kN.s/m)	γC_i (kN.s/m)
3	0.62	0.62	0.219			0.183	0.73	0.58
2	0.84	1.46	0.740			0.438	1.35	1.08
1	0.46	1.92	1.101			0.576	1.42	1.14
Base				1.69	0.84			

Table 5. Member and damper design parameters for the 6-story structure.

Level	F_i (kN)	V_i (kN)	$M_{b,i}$ (kN.m)	$M_{col,int}$ (kN.m)	$M_{col,ext}$ (kN.m)	F_{di} (kN)	Ci (kN.s/m)	γC_i (kN.s/m)
6	0.32	0.32	0.115			0.096	0.82	0.49
5	0.52	0.84	0.419			0.254	1.87	1.12
4	0.44	1.28	0.766			0.386	2.51	1.51
3	0.35	1.63	1.05			0.491	2.86	1.72
2	0.24	1.87	1.26			0.565	2.98	1.79
1	0.13	2	1.28			0.604	2.83	1.70
Base				1.78	0.89			

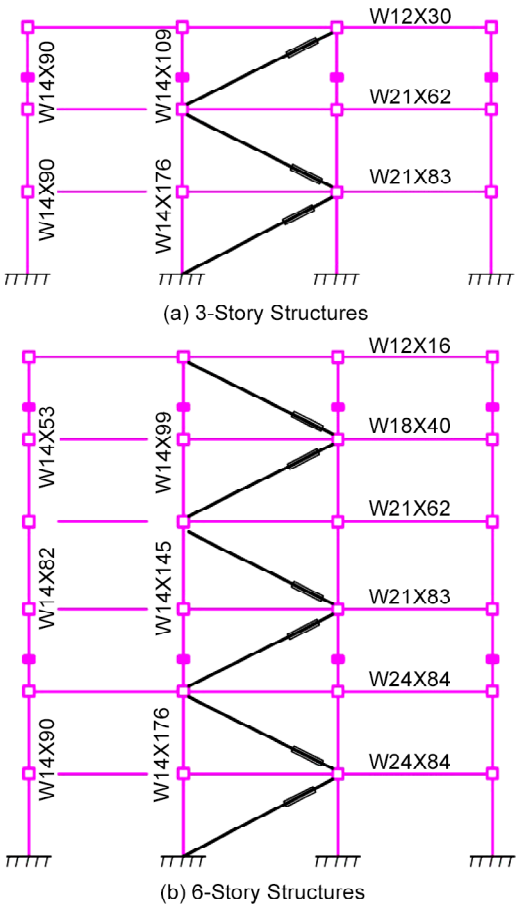

Figure 6. Member sizes for the designed.

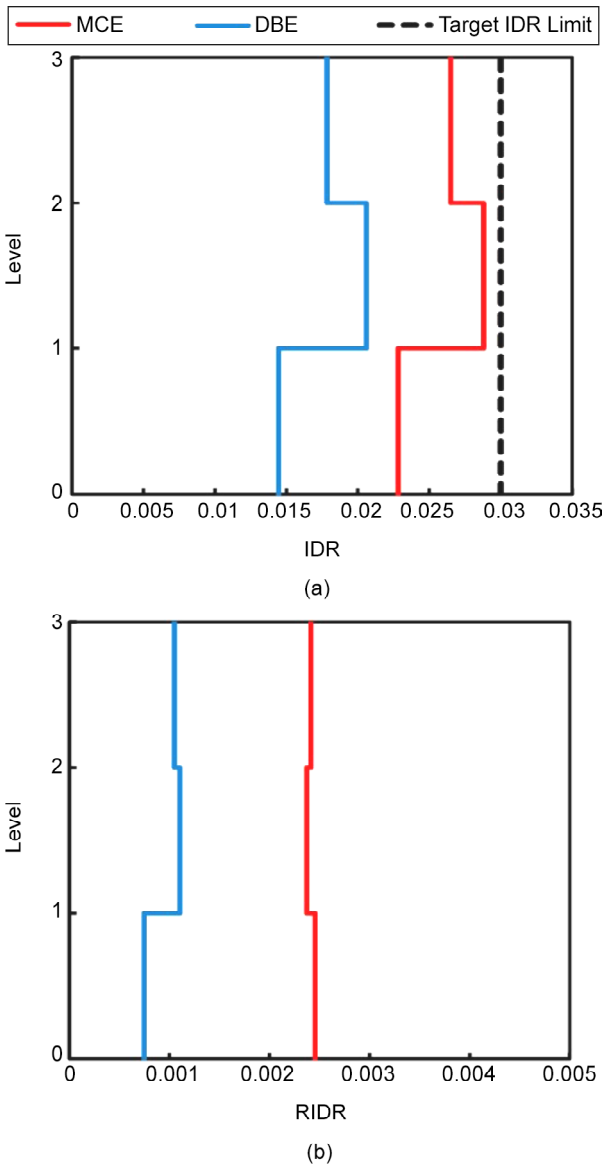

Figure 7. Nonlinear responses for (a) the mean IDRs and (b) the median RIDRs at the DBE and MCE levels for the 3-story structure without considering the composite action.

5. Results of Nonlinear Dynamic Analyses

After modeling the structures in the OpenSees program with the above-mentioned details, nonlinear dynamic time history analyses were performed to obtain the values of mean IDR and the values of median RIDR. The maximum value of mean IDRs in each structure corresponds to the performance level of the structure. Furthermore, the maximum value of median RIDRs indicates the damage states of the structures. It is worth noting that because the FEMA P58 (2018) damage states were implemented to quantify the damages, the values of median RIDR instead of the values of mean RIDR were used in this paper.

In this section, the results of the mentioned parameters for two cases that include considering and neglecting the effect of composite action, are presented and discussed.

Figure (7a) gives the values of IDR for the 3-story structure without considering the effect of composite action at both the DBE and MCE hazard levels. As can be seen, this structure could acceptably satisfy the target IDR limit of 3.0% at the MCE level. Moreover, the maximum value of 2.06% for the mean IDRs is obtained at the DBE level, which is lower than the allowable value of 2.5% proposed by Sullivan et al. (2012) for the life safety performance level. On the other hand, for the median RIDRs demand, as shown in Figure (7b), the maximum values of 0.11% and 0.24% are achieved at the DBE and MCE levels, respectively. According to FEMA P58, the mentioned structure satisfies design stage 1 (DS-1) at the DBE level. This means that although the structure does not need any structural realignment, some non-structural components may require repairs. Also, since the maximum value of median RIDRs at the MCE level slightly exceeds the value

of 0.2% (limit state for DS-1 = 0.2%), the damage state for the structure is classified as DS-1 to less than DS-2, according to FEMA P-58. Therefore, the 3-story structure designed by the DDBD method seems to have acceptable seismic behavior at both the hazard levels.

The values of mean IDR for the 6-story structure without considering the effect of composite action are given in Figure (8a) at the two hazard levels. It can be observed from this figure that the maximum value of mean IDRs is equal to 2.8% at the MCE level. Furthermore, the maximum value of mean IDRs at the DBE level is under the limit of the life safety performance level (i.e., 2.5%). Although the maximum value of median RIDRs at MCE level increases from 0.24% to 0.4% compared with the 3-story structure, the mentioned value is still under 0.5% (i.e., DS-1 to less than DS-2), as depicted in Figure (8b). Moreover, the structure could acceptably satisfy the DS-1 at the DBE level.

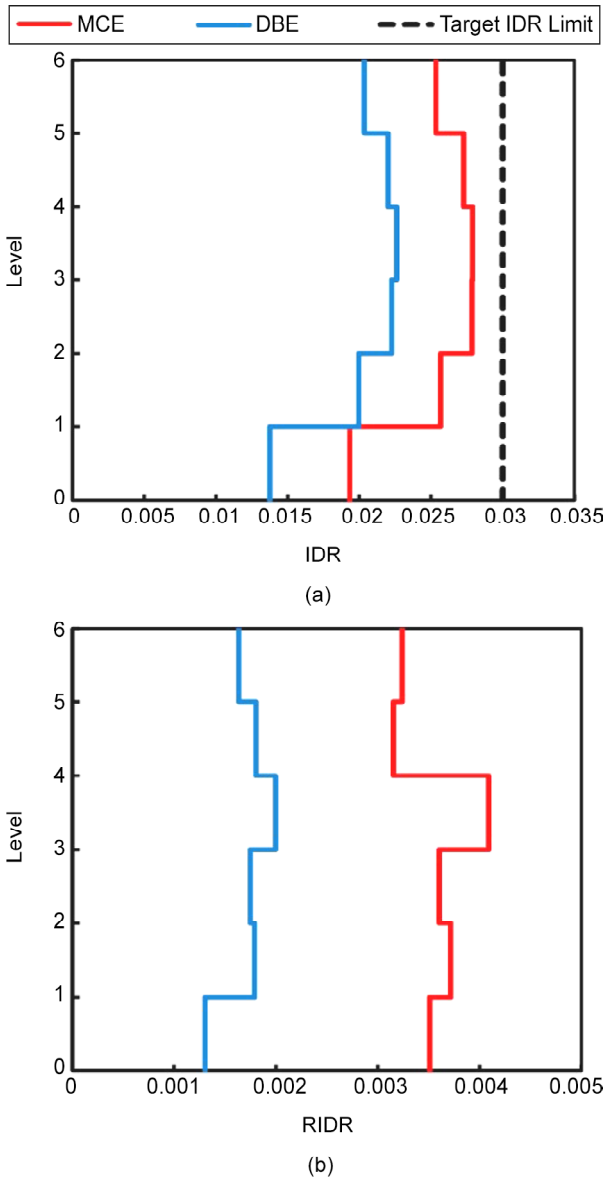

Figure 8. Nonlinear responses for (a) the mean IDRs and (b) the median RIDRs at the DBE and MCE levels for the 6-story structure without considering the composite action.

As discussed before, the results of nonlinear analyses for the structures subjected to ground motions were presented for the case of neglecting the effect of composite action. While considering the effect of composite action, the periods of the structures change. In fact, the flexural strength of shear tab connections and the effect of slab concrete increase the strength and stiffness of the structures. Figure (9) compares the period of the structures with and without the effect of composite action. It is noted that W/O and W stand for without and with, respectively, in all the following figures. It can be seen that the fundamental period of the 3-story and 6-story structures reduces by 7.0% and 12%, respectively.

The effect of considering composite action on the mean IDR and the median RIDR profile values

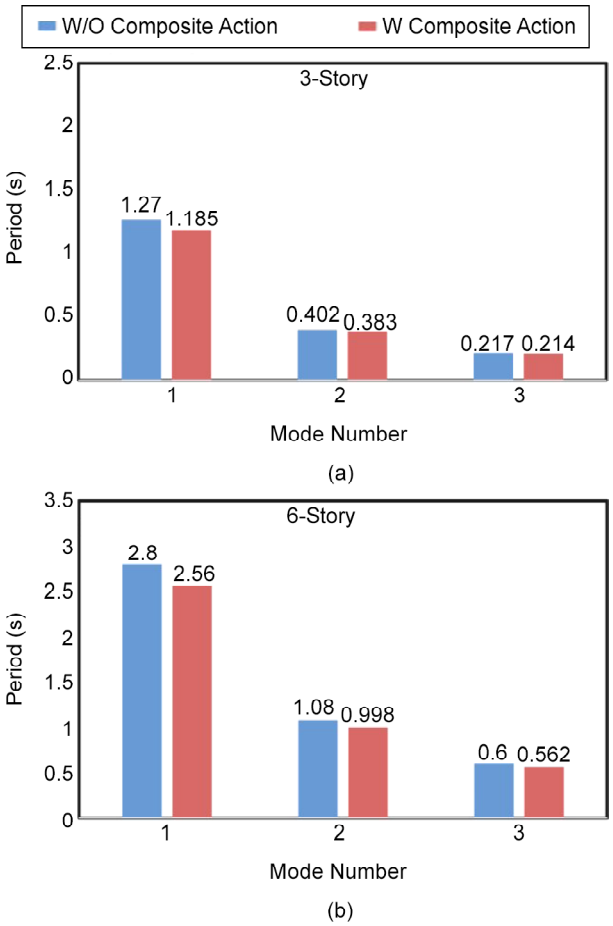

Figure 9. Comparing the period of (a) 3-story and (b) 6-story structures with and without considering the composite action.

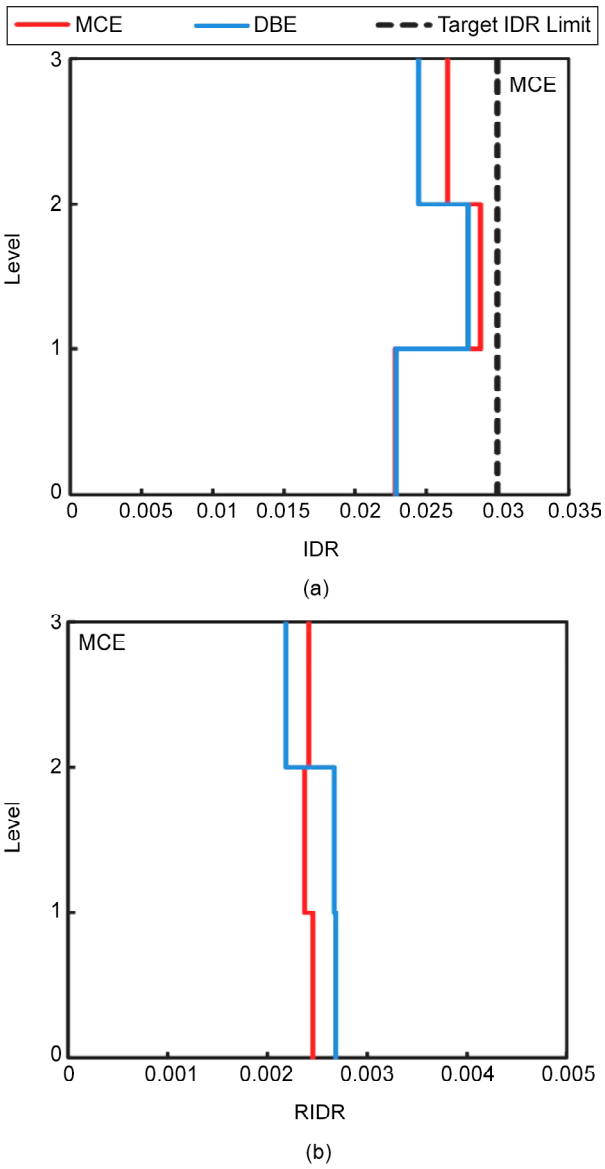

Figure 10. Nonlinear responses for (a) the mean IDRs and (b) the median RIDRs at the MCE level for the 3-story structure with considering the composite action.

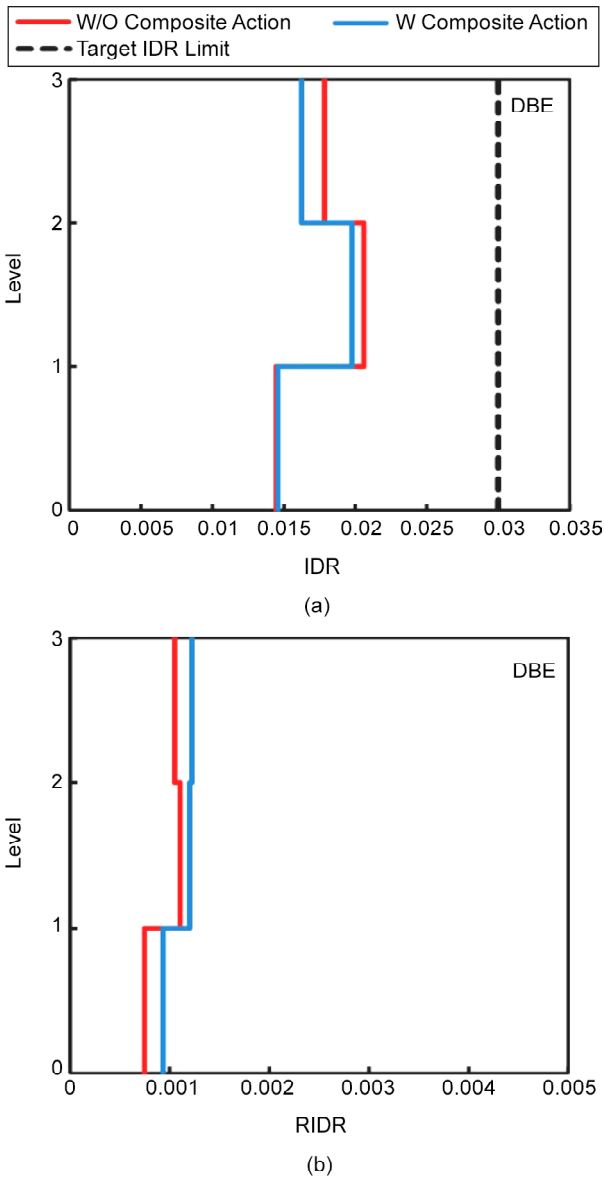

Figure 11. Nonlinear responses for (a) the mean IDRs and (b) the median RIDRs at the DBE level for the 3-story structure with considering the composite action.

is shown in Figures (10) and (11) for the 3-story structure at the DBE and MCE levels, respectively. According to these figures, a slight reduction of approximately 4% occurs in the maximum value of mean IDRs at both the DBE and MCE levels. In contrast with the mean IDR profile values, an increase of about 9% is seen in the maximum value of median RIDRs at both the MCE and DBE hazard levels.

Similar trends are observed for the mean IDR and the median RIDR profile values in the 6-story structure compared to the 3-story structure, as shown in Figures (12) and (13). According to the obtained results, it can be inferred that considering the composite action increases the stiffness (reduction in fundamental period) and strength of the structures. Thus, the structures can attract more forces during the earthquake compared with those that neglect this effect. Lower profile values of the mean IDR at both the DBE and MCE levels indicate the effect of composite action when compared to the case in which the effect was neglected. It is worth noting that the presence of dampers reduces the significance of the composite action. On the other hand, although the composite action enhances the stiffness and strength of the structures, the median RIDR profile values are also increased. It is evident that the IDR and RIDR parameters relate to the seismic performance of the structures, but the character of these parameters

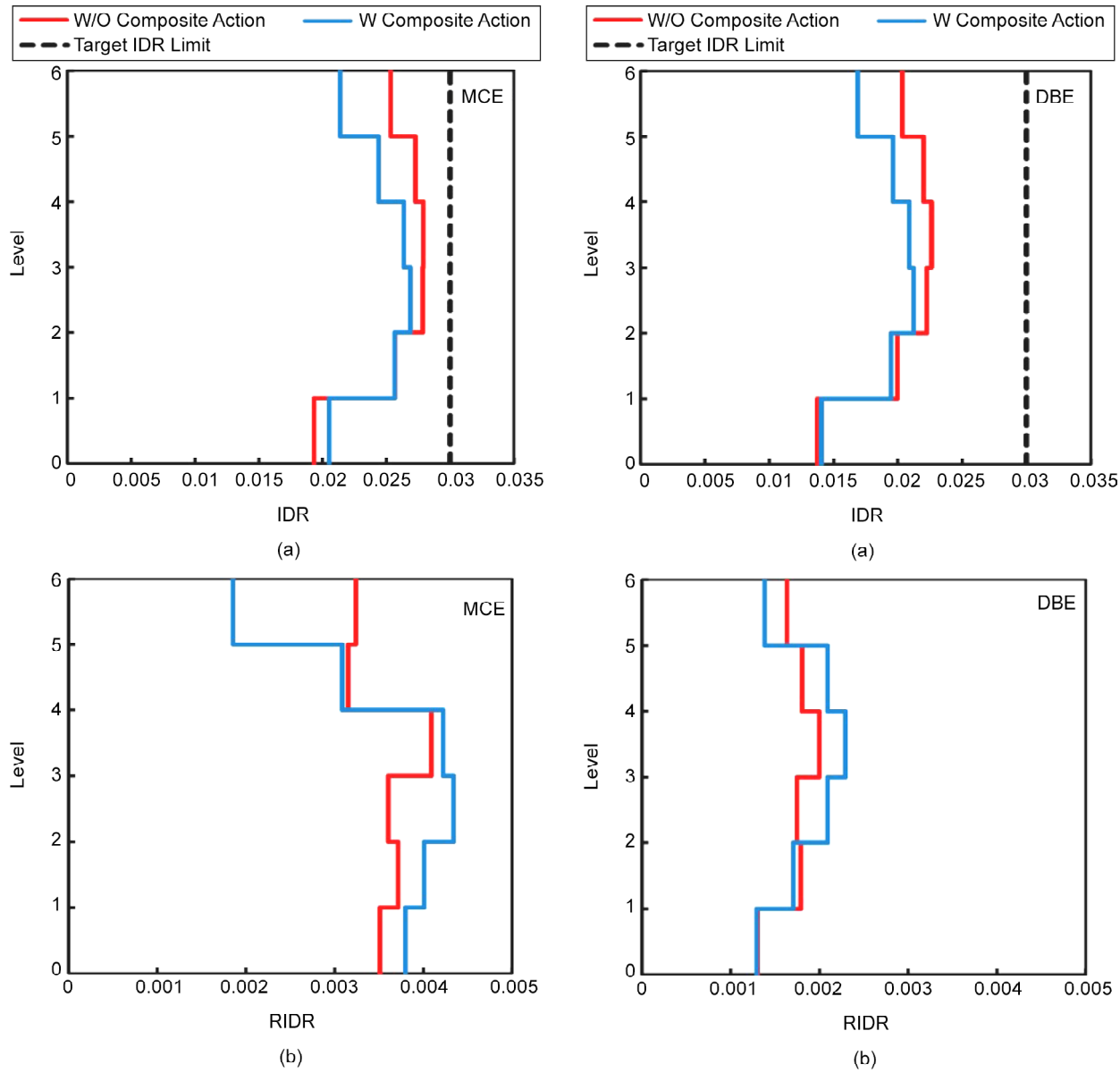

Figure 12. Nonlinear responses for (a) the mean IDRs and (b) the median RIDRs at the MCE level for the 6-story structure with considering the composite action.

Figure 13. Nonlinear responses for (a) the mean IDRs and (b) the median RIDRs at the DBE level for the 6-story structure with considering the composite action.

is different. The parameter RIDR is determined at the end of an earthquake (after free vibration of the structure) and the cyclic deterioration affects this parameter. The reason for the increase in the median RIDR profile values in the case of considering the composite action can be related to concrete slab crushing. In other words, the effect of composite action causes an enhancement in the flexural stiffness and strength of the structures, so the structures attract more forces, while these extra forces lead to concrete slab crushing and more cyclic deterioration at the end of an earthquake. Therefore, higher median RIDR profile values are achieved. It should be mentioned that the results of the analyses in this paper are dependent on the number of stories, concrete slab thickness, rib thickness, etc. Investigating the effect of the mentioned parameters on the RIDR values is proposed for future research studies. In addition, in most of the forced-based design methods, the composite action is not considered in the design procedure. However, different research studies, such as Elkady and Lignos (2014), Hwang & Lignos (2017) and Yakhchalian and Yakhchalian (2023), have shown that this effect can considerably affect the seismic engineering demand parameters. The aim of this study is to reveal how much this affects the seismic responses in the steel MRFs

with dampers designed with the modified DDBD method. As shown, this can affect the results. Therefore, in future research studies, methods of considering this effect in the design process or modifying evaluations can be developed in such a way as to include this effect.

6. Conclusions

This paper investigated the effect of modeling composite action on the seismic performance of mid-rise steel MRFs with linear fluid viscous dampers designed by the modified DDBD method. Nonlinear dynamic time history analyses were performed for the 3-story and 6-story structures subjected to 20 ground motion records at two seismic hazard levels. The effects of modeling panel zone flexibility and gravity framing were also considered in the analyses, whereas fewer research studies have been made on the mentioned effects in the framework of the DDBD method. The results of analyses were obtained based on two cases, involving considering and neglecting the effect of composite action on the gravity framing and beam elements of the MRF. The seismic performance level of the designed structures corresponds to the maximum value of mean IDRs at each hazard level, separately. Furthermore, the maximum value of median RIDRs indicates the intensity of required repair for the structures according to FEMA P58. The following results can be summarized:

1. The modified DDBD method could acceptably satisfy the assumed performance level for the designed structures in both cases, considering and neglecting the composite action.
2. Considering the composite action increases the initial stiffness of structures and this effect reduced the fundamental period of the structures. The fundamental period is reduced by 7.0% and 12.0% in the 3- and 6-story structures, respectively, in comparison with the cases in which the composite action was neglected.
3. The maximum value of mean IDRs at the MCE hazard level was obtained equal to 2.9% and 2.8% for the 3- and 6-story structures, respectively, when the composite action was not considered. These values decreased to 2.8% and 2.7%, respectively, when the composite action was considered.
4. Accounting for the composite action in the nonlinear dynamic analyses led to a higher maximum value of median RIDRs in comparison with the case where this effect was not considered. This enhancement is more noticeable at the MCE level than at the DBE level. More cyclic deterioration as well as concrete slab crushing at the MCE level resulted in higher median RIDR profile values.
5. According to FEMA P58, the 3-story structure was classified as DS-1 and DS-2 with and without considering the composite action at the DE and MCE hazard levels, respectively. For the 6-story structure, considering the composite action changed the damage stage based on the median RIDR profile values from DS-1 to DS-2 at the DBE hazard level. Considering or neglecting the mentioned effect did not affect the damage stage of the structure at the MCE hazard level.

References

Alehojjat, S. B., Bahar, O., & Yakhchalian, M. (2021). Improvements in the direct displacement-based design procedure for mid-rise steel MRFs equipped with viscous dampers. *Structures*, *34* (August), 1636-1650. doi: 10.1016/j.istruc.2021.08.047

Alehojjat, S. B., Yakhchalian, M., & Bahar, O. (2023). Approximate methods to estimate residual drift demands in steel structures with viscous dampers designed by the DDBD approach. *International Journal of Steel Structures*, *23*(3), 806-822. doi: 10.1007/s13296-023-00732-4

Alehojjat, S. B., Yakhchalian, M., & Bahar, O. (2024). Seismic performance assessment of mid-rise steel structures with dampers designed by the modified DDBD method. *9th International Conference on Seismology and Earthquake Engineering*, Tehran, Iran.

Arab, R., & Yakhchalian, M. (2022). Investigating approximate methods to predict residual interstory drift ratio demands in steel eccentrically braced frames. *International Journal of Steel Structures*, *22*(1), 176-191. doi: 10.1007/s13296-021-00565-z

ASCE 41. (2017). *Seismic Evaluation and Retrofit*

of Existing Buildings, Reston, VA: American Society of Civil Engineers.

ASCE 7. (2017). *Minimum Design Loads for Buildings and Other Structures*. Reston, VA: American Society of Civil Engineers.

Asgarkhani, N., Yakhchalian, M., & Mohebi, B. (2020). Evaluation of approximate methods for estimating residual drift demands in BRBFs. *Engineering Structures*, *224*(April), 110849. doi: 10.1016/j.engstruct.2020.110849

Elkady, A. (2022). FM-2D: Open-Source platform for the numerical modeling and seismic analysis of buildings. *SoftwareX*, *17*(1), doi: 10.1016/j.softx.2021.100927

Elkady, A., & Lignos, D. G. (2014). Modeling of the composite action in fully restrained beam-to-column connections: implications in the seismic design and collapse capacity of steel special moment frames. *Earthquake Engineering and Structural Dynamics*, *43*(13), 1935-1954. doi: 10.1002/eqe.2430

Elkady, A., & Lignos, D. G. (2015). Effect of gravity framing on the overstrength and collapse capacity of steel frame buildings with perimeter special moment frames. *Earthquake Engineering and Structural Dynamics*, *44*(8), 1289-1307. doi: 10.1002/eqe.2519

Erochko, J., Christopoulos, C., Tremblay, R., & Choi, H. (2011). Residual drift response of SMRFs and BRB frames in steel buildings designed according to ASCE 7-05. *Journal of Structural Engineering*, *137*(5), 589-599. https://ascelibrary.org/doi/abs/10.1061/%28ASCE%29ST.1943-541X.0000296

Farahani, S., & Akhaveissy, A. H. (2022). Direct displacement-based seismic design of buckling-restrained braced RC frames. *Bulletin of Earthquake Engineering*, *20*(3), 1767-1839. doi: 10.1007/s10518-021-01290-y

FEMA (2018). *Seismic Performance Assessment of Buildings, Vol 1: Methodology, Second Edition*. FEMA P-58-1 Washington DC: Federal Emergency Management Agency.

Green, T., Leon, R., & Rassati, G. (2004). Bidirectional tests on partially restrained, composite beam-to-column connections. *Journal of Structural Engineering*, *130*(2), 320-327. doi: 10.1061/(ASCE)0733-9445(2004)130:2(320)

Gupta, A., & Krawinkler, H. (1999). *Seismic Demands for the Performance Evaluation of Steel Moment Resisting Frame Structures*. Report No. 132. The John A. Blume Earthquake Engineering Center, Stanford University, CA.

Hu, S., Zhang, R., & Wang, W. (2023). Hybrid self-centering dual rocking core system for seismic resilience by controlling both structural and nonstructural damage. *Engineering Structures (Online)*, *295*, 116796. doi: 10.1016/j.engstruct.2023.116796

Hwang, S., & Lignos, D. G. (2017). Earthquake-induced loss assessment of steel frame buildings with special moment frames designed in highly seismic regions. *Earthquake Engineering & Structural Dynamics*, *46*(13), 2141-2162. doi: 10.1002/eqe.2898

Ibarra, L. F., Medina, R. A., & Krawinkler, H. (2005). Hysteretic models that incorporate strength and stiffness deterioration. *Earthquake Engineering & Structural Dynamics*, 34(12), 1489-1511. doi: 10.1002/eqe.495

Kalapodis, N. A., Muho, E. V., & Beskos, D. E. (2022). Seismic design of plane steel MRFS, EBFS and BRBFS by improved direct displacement-based design method. *Soil Dynamics and Earthquake Engineering*, *153*, 107111. doi: 10.1016/j.soildyn.2021.107111

Kitayama, S., & Constantinou, M. C. (2016). *Development and Evaluation of Procedures for Analysis and Design of Buildings with Fluid Self-Centering Systems, MCEER-16-0003*.

Kitayama, S., & Constantinou, M. C. (2018). Collapse performance of seismically isolated buildings designed by the procedures of ASCE/SEI 7. *Engineering Structures*, *164*(March), 243-258. doi: 10.1016/j.engstruct.2018.03.008

Leon, R., Hajjar, J., & Gustafson, M. (1998). Seismic response of composite moment-resisting connections, I: performance. *Journal of Structural Engineering*, *124*(8), 868-876. doi: 10.1061/(ASCE)0733-9445(1998)124:8(868).

Lignos, D. G., & Krawinkler, H. (2011). Deterioration modeling of steel components in support of

collapse prediction of steel moment frames under earthquake loading. *Journal of Structural Engineering*, *137*(11), 1291-1302. doi: 10.1061/(ASCE)ST.1943-541X.0000376

Lignos, D. G., Hartloper, A., Elkady, A., Deierlein, G. G., & Hamburger, R. (2019). Proposed updates to the ASCE 41 nonlinear modeling parameters for wide-flange steel columns in support of performance-based seismic engineering. *Journal of Structural Engineering*, *145*(9):04019083. doi: 10.1061/(ASCE) ST.1943-541X.0002353

Liu, J., & Astaneh-Asl, A. (2000). Cyclic testing of simple connections including effects of slab. *Journal of Structural Engineering*, *126*(1), 32-39. doi: 10.1061/(ASCE)0733-9445(2000)126:1(32)

Liu, J., & Astaneh-Asl, A. (2004). Moment-rotation parameters for composite shear tab connections. *Journal of Structural Engineering*, *130*(9), 1371-1380, doi: 10.1061/(ASCE)0733-9445(2004)130:9(1371)

Moradpour, S., & Dehestani, M. (2019). Optimal DDBD procedure for designing steel structures with nonlinear fluid viscous dampers. *Structures*, *22* (August), 154-174. doi: 10.1016/j.istruc.2019.08.005

Noruzvand, M., Mohebbi, M., & Shakeri, K. (2020). Modified direct displacement-based design approach for structures equipped with fluid viscous damper. *Structural Control and Health Monitoring*, *27*(1), 1-19. doi: 10.1002/stc.2465

Noruzvand, M., Mohebbi, M., & Shakeri, K. (2021). An improvement of direct displacement-based design approach for steel moment-resisting frames controlled by fluid viscous dampers. *Advances in Structural Engineering*, 136943322199249. doi: 10.1177/1369433221992496

OpenSees (2020). *Open System for Earthquake Engineering Simulation*. Pacific Earthquake Engineering Research Center, Berkeley, CA. http://opensees.berke ley.edu

Papagiannopoulos, G. A., Hatzigeorgiou, G. D., & Beskos, D. E. (2013). Recovery of spectral absolute acceleration and spectral relative velocity from their pseudo-spectral counterparts. *Earthquake and Structures*, *4*(5), 489-508. doi: 10.12989/eas.2013. 4.5.489

Priestley, M. J. N., Calvi, G. M., & Kowalsky, M. (2007). *Displacement Based Seismic Design of Structures*. IUSS Press.

Priestley, N. M. J. (1993). Myths and fallacies in earthquake engineering-conflicts between design and reality. *Bulletin of the New Zealand National Society for Earthquake Engineering*, *26*(3), 329-341. doi: 10.5459/bnzsee.26.3.329-341

Rahgozar, N., & Rahgozar, N. (2020). Extension of direct displacement-based design for quantifying higher mode effects on controlled rocking steel cores. *The Structural Design of Tall and Special Buildings*, *29*(16). doi: 10.1002/tal.1800

Shakeri, K., & Dadkhah, H. (2021). Development of DDBD for steel MRFs using inelastic response-based seismic lateral force distribution. *Journal of Building Engineering*, *43*, 103063. doi: 10.1016/j.jobe.2021. 103063

Somerville, P. G. (1997). Development of ground motion time histories for phase 2 of the FEMA/SAC steel project. SAC Joint Venture.

Sullivan, T. J., & Lago, A. (2012). Towards a simplified Direct DBD procedure for the seismic design of moment resisting frames with viscous dampers. *Engineering Structures*, *35*, 140-148. doi: 10.1016/j.engstruct.2011.11.010

Sullivan, T. J., Priestley, M. J. N., & Calvi, G. M. (Eds.). (2012). *A Model Code for the Seismic Design of Structures, DBD12*. IUSS Press.

Sullivan, T. J., Saborio-Romano, D., O'Reilly, G. J., Welch, D. P., & Landi, L. (2018). Simplified pushover analysis of moment resisting frame structures. *Journal of Earthquake Engineering*, *25*(4), 621-648. doi: 10.1080/13632469.2018.1528911

Yakhchalian, M. & Yakhchalian, M., (2023). Gravity framing and composite action effects on residual drifts of steel SMFs. *Journal of Constructional Steel Research*, *211*, 108167. doi: 10.1016/j.jcsr.2023.108167